

Effect of cluster-shell competition of ^{12}C on $E0$ transitions in ^{16}O

H. Matsuno¹ and N. Itagaki²

¹*Department of Physics, Kyoto University,*

Kitashirakawa Oiwake-Cho, Kyoto 606-8502, Japan

²*Yukawa Institute for Theoretical Physics, Kyoto University,*

Kitashirakawa Oiwake-Cho, Kyoto 606-8502, Japan

(Dated: June 8, 2021)

In ^{16}O , we investigate the relation between the $E0$ monopole transition matrix elements and cluster-shell competition using antisymmetrized quasi cluster model (AQCM), where the dissolution of α clusters into quasi clusters due to the effect of the spin-orbit force is introduced. We focus on the structure change when the strength of the spin-orbit force is varied. The ground state dominantly has a compact four α structure (doubly magic structure of the p shell), which is rather independent of the strength. However the first excited state (0_2^+) has $^{12}\text{C} + \alpha$ cluster structure and this state is largely affected by the increase of the strength; the subclosure configuration of the $p_{3/2}$ shell for the ^{12}C cluster part becomes more important than three α configuration. The $E0$ transition from the ground state with compact four α configuration to the 0_2^+ state with $^{12}\text{C} + \alpha$ cluster configuration is suppressed when increasing the spin-orbit strength. Although the $E0$ operator itself does not have the spin dependence, the matrix element is sensitive to the difference of intrinsic spin structures of the two states. The $E0$ transition characterizes the persistence of four α structure in the 0_2^+ state.

PACS numbers: 21.60.Gx, 21.10.Ky

I. INTRODUCTION

The $E0$ monopole transition has been regarded as a physical quantity which is related to the matter properties of heavy nuclei. In addition, recently it has been discussed that it is closely related to the structures of light nuclei, especially for their cluster structure [1]. The $E0$ monopole excitation induces the breathing mode of nuclei. However changing nuclear density requires highly excitation energy because of the saturation property of nuclear systems. On the other hand, if the system is composed of strongly bound subsystems called clusters, the relative interaction between cluster is weak, and it is possible to change the relative distances (nuclear sizes) without giving high excitation energies. α clusters are very stable and they are good candidates. The monopole excitation is expected to induce α cluster excitation (excitation from the ground state to states with α cluster structure) in low excitation energy region. Indeed, strong monopole transition and the relation to α clustering have been discussed in ^{10}B [1], $^{12,13}\text{C}$ [2–4], and ^{24}Mg *etc* [5, 6].

Now we focus on the case that the counterpart of the α cluster has more complex structure. There have been numerous works showing that the low-lying states of ^{16}O , including the 0_2^+ state, have $^{12}\text{C} + \alpha$ structure [7–9]. Also in this nucleus, the $E0$ strength distribution has been observed [10]. If we compare the results with the random phase approximation (RPA) calculation based on the mean-field theory [11], the agreement in high excitation energy region is good; however it is not in low excitation energy region. There some of the strong peaks observed are missing in the calculation. For example, the $E0$ transitions from the 0_1^+ to the 0_2^+ and 0_3^+ states are observed to be $3.55 \pm 0.21 e\text{fm}^2$ and $4.03 \pm 0.09 e\text{fm}^2$, respectively [12, 13], and they correspond to about 3%

and 8% of the energy weighted sum rule [14]. Based on the cluster approaches, these $E0$ transitions to low-lying states are theoretically explained in the frameworks of $^{12}\text{C} + \alpha$ orthogonality condition model (OCM) [15], 4α OCM [16] and ^{12}C (antisymmetrized molecular dynamics: AMD) + α generator coordinate method (GCM) [17]. Yamada *et al.* pointed out in Ref. [14] that there are two reasons for the $E0$ transition from the ground state to low-lying cluster states. One is the duality; simple shell model wave function automatically contains the clustering degree of freedom. If we take the zero limit for the relative distance between ^{12}C and α , the wave function agrees with the closed p shell configuration of the shell model. Thus there is certain path from the ground state to the $^{12}\text{C} + \alpha$ cluster configuration. This is explained by the so-called Bayman-Bohr theorem [18]. The other is ground state correlation. The ground state slightly deviates from the shell model limit and contains more $^{12}\text{C} + \alpha$ cluster configurations when the wave functions corresponding to this path are superposed. This effect enhances the transition from the ground state to the $^{12}\text{C} + \alpha$ cluster states.

However, the discussion of Bayman-Bohr theorem is based on the three-dimensional harmonic oscillator type wave function (or $N\alpha$ cluster model wave function with some limit of relative distances) and it is not trivial whether the same logic holds or not when the jj -coupling shell model wave functions are introduced. The ground state is rather safe; the closed p shell configuration, which plays a dominant role in the ground state, can be equally described by the four α cluster model and jj -coupling shell model. On the contrary, there appears non-negligible difference in the wave function of $^{12}\text{C} + \alpha$ states when the jj -coupling ^{12}C is introduced. In our previous analysis for ^{12}C , we discussed that the ground

state of ^{12}C is an intermediate state between three α cluster state and the subclosure configuration of $p_{3/2}$ in the jj -coupling shell model, and there the contribution of the spin-orbit force is quite strong [19]. In ^{16}O , both wave functions of the ground and excited states contribute to the monopole transition matrix elements, and it is worthwhile to investigate whether the inclusion of shell model like wave functions for the ^{12}C cluster part changes the story of monopole transition strengths in the low energy regions or not.

In this paper, we discuss the behavior of the $E0$ transition matrix elements from the ground state when the jj -coupling shell model ^{12}C is mixed with three α in the excited states of ^{16}O . We take notice on the $E0$ transition matrix elements as a function of the strength of the spin-orbit force in the Hamiltonian. With increasing the spin-orbit strength, the α breaking components become more important, and jj -coupling shell model ^{12}C strongly mixes in the $^{12}\text{C}+\alpha$ cluster states. Although the $E0$ operator itself does not have the spin dependence, the $E0$ transition matrix elements turns out to be sensitive to this change.

As a theoretical framework, we use antisymmetrized quasi cluster model (AQCM) [19–22]. AQCM is the method, which can describe jj -coupling shell model wave function by extending cluster model. The remarkable advantage of AQCM is that the number of the parameters required to characterize the transition from cluster state to jj -coupling shell state is quite small. In addition to the distance parameters used in traditional cluster models, AQCM needs only one new parameter Λ , which describes the dissolution of α clusters and change into jj -coupling shell state; the clusters with finite Λ value are called “quasi clusters”. In ^{12}C , Suhara *et al.* were successful to describe the change of three α cluster state into the $p_{3/2}$ subclosure configuration of the jj -coupling shell model with only two parameters, namely distance parameter R and dissolution parameter Λ [19]. In this work, we adopt the method to describe the ^{12}C part of the $^{12}\text{C} + \alpha$ cluster states in ^{16}O .

This paper is organized as follows. We explain our formulation for this work in Sec. II. The results and discussion are given in Sec. III. Finally, we present conclusion and outlook in Sec. IV.

II. FORMULATION

In this section, we explain the wave function and Hamiltonian in our model.

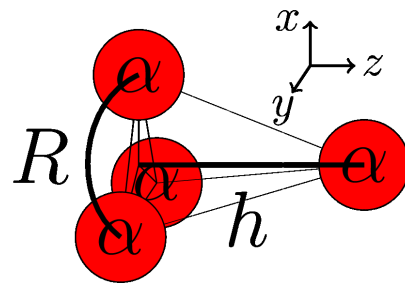


FIG. 1: (Color online) The schematic figure for the definitions of R and h . The red spheres show the α clusters and three of them on the x - y plane are changed into quasi clusters.

A. Wave function

1. Single-particle wave function

The single-particle wave function is described by Gaussian packet,

$$\phi_i = \left(\frac{2\nu}{\pi}\right)^{\frac{3}{4}} \exp[-\nu(\mathbf{r} - \boldsymbol{\zeta}_i)^2] \chi_i \tau_i, \quad (1)$$

where χ_i and τ_i are spin and isospin part of the i th single-particle wave function, respectively. For the width parameter ν ($= 1/2b^2$), we use the value of $b = 1.6$ fm to reproduce the radius of ^{16}O . If we choose the same Gaussian center parameter ζ_i for four nucleons (spin up proton, spin down proton, spin up neutron and spin down neutron), the four nucleons are regarded as forming an α cluster.

The coordinate system is defined in the following way. Firstly, we place three α clusters on the x - y plane in regular triangle shape, which are regarded as ^{12}C cluster. The length of one side is defined as R . Secondly, we place the fourth α cluster on the z axis. The length between the center of masses of the fourth α cluster and ^{12}C is defined as h . If $h = \sqrt{2/3} \times R$, the four α clusters configure tetrahedron shape. The definitions of R and h are schematically shown in Fig. 1. Thirdly, we introduce a dissolution parameter Λ for the three α clusters on the x - y plane. For the details of introducing Λ for ^{12}C , see Ref. [19]. Finally, the center of gravity of the whole system is moved to the origin.

2. Wave function of the total system

The wave function of the total system is parity and angular momentum eigenstate:

$$\Phi = \sum_{i,j,k} c_{ijk} \Psi_{ijk}, \quad (2)$$

$$\begin{aligned} \Psi_{ijk} &= \Psi(R_i, h_j, \Lambda_k) \\ &= \hat{P}_{MK}^J \hat{P}^\pi \mathcal{A}[\phi_1 \cdots \phi_{16}], \end{aligned} \quad (3)$$

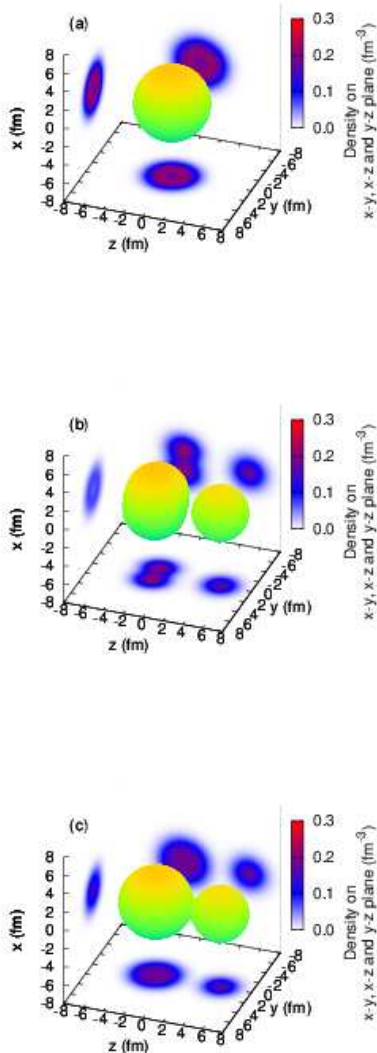


FIG. 2: (Color online) Intrinsic density distributions of typical basis states. The nuclear surface is defined as the point with the density of 0.01 fm^{-3} . Right back, left back and bottom figures are density distributions on the x - z plane, x - y plane and y - z plane, respectively. These parameters are (a) $R = 0.1 \text{ fm}$, $h = \sqrt{2/3} \times 0.1 \text{ fm}$, $\Lambda = 0$, (b) $R = 0.1 \text{ fm}$, $h = \sqrt{2/3} \times 8.0 \text{ fm}$, $\Lambda = 0$ and (c) $R = 0.1 \text{ fm}$, $h = \sqrt{2/3} \times 8.0 \text{ fm}$, $\Lambda = 1$.

where \hat{P}_{MK}^J and \hat{P}^π are angular momentum projection operator and parity projection operator, respectively. \mathcal{A} is antisymmetrizer for all sixteen nucleons. The parameters are taken as $\{R_i\} = 0.1, 1.0, 2.0, 3.0, 4.0 \text{ fm}$, $\{h_j\} = \sqrt{2/3} \times (0.1, 1.0, 2.0, 3.0, 4.0, 5.0, 6.0, 7.0, 8.0) \text{ fm}$ and $\{\Lambda_k\} = 0, 1/3, 2/3, 1$, respectively. There are $5 \times 9 \times 4 = 180$ bases and the coefficient c_{ijk} is determined by solving the Hill-Wheeler equation.

The intrinsic density distributions (*i.e.* the density distributions before angular momentum and parity projections) of typical basis states are shown in Fig. 2. In Fig. 2 (a), the four α clusters configure compact tetrahedron shape, and parameters are set to $R = 0.1 \text{ fm}$, $h = \sqrt{2/3} \times 0.1 \text{ fm}$ and $\Lambda = 0$. In this case, the density looks having a spherical symmetry. This state corresponds to the $(0s)^4(0p)^{12}$ closed shell configuration at the limit of $h = \sqrt{2/3} \times R \rightarrow 0$ as described in the so-called Bayman-Bohr theorem [18]; the zero limit for the distances between α clusters with certain shape corresponds to the closed-shell configurations. Figure 2 (b) and (c) show the $^{12}\text{C} + \alpha$ cluster like states, where the parameter h is increased to $h = \sqrt{2/3} \times 8.0 \text{ fm}$, while keeping $R = 0.1 \text{ fm}$. In Fig. 2 (b) and (c), ^{12}C cluster is put on the left-hand side and the last α cluster is on the right-hand side. In Fig. 2 (b), the dissolution parameter is set to $\Lambda = 0$ and ^{12}C cluster is nothing but three α clusters. In Fig. 2 (c), the dissolution parameter is set to $\Lambda = 1$ and three α clusters in ^{12}C are changed into quasi clusters, which correspond to the subclosure configuration of $p_{3/2}$ at the limit of $R \rightarrow 0$. Here, the density of the ^{12}C cluster part looks having a spherical symmetry.

B. Hamiltonian

The Hamiltonian used in our work is given as

$$\hat{H} = \hat{T} - \hat{T}_G + \hat{V}_C + \hat{V}_{\text{LS}} + \hat{V}_{\text{Coulomb}}, \quad (4)$$

where \hat{T} is total kinetic energy operator and \hat{T}_G is kinetic energy of center of mass motion. We use the Volkov No.2 [23] for the central force \hat{V}_C :

$$\hat{V}_C = \sum_{i < j}^A \left[V_a \exp\left(-\frac{\hat{r}_{ij}^2}{\alpha^2}\right) + V_r \exp\left(-\frac{\hat{r}_{ij}^2}{\rho^2}\right) \right] \times \left[W + B \hat{P}_{ij}^\sigma - H \hat{P}_{ij}^\tau - M \hat{P}_{ij}^\sigma \hat{P}_{ij}^\tau \right], \quad (5)$$

where $V_a = -60.65 \text{ MeV}$, $V_r = 61.14 \text{ MeV}$, $\alpha = 1.80 \text{ fm}$ and $\rho = 1.01 \text{ fm}$ are original values and we adopt $M = 1 - W = 0.62$ and $B = H = 0.125$. We use spin-orbit part of G3RS force [24] for \hat{V}_{LS} :

$$\hat{V}_{\text{LS}} = \sum_{i < j}^A \left[V_{\text{LS1}} \exp\left(-\frac{\hat{r}_{ij}^2}{\eta_1^2}\right) + V_{\text{LS2}} \exp\left(-\frac{\hat{r}_{ij}^2}{\eta_2^2}\right) \right] \times \hat{P}_{ij}(^3O) \hat{\mathbf{L}}_{ij} \cdot \hat{\mathbf{S}}_{ij}, \quad (6)$$

where $\eta_1 = 0.447 \text{ fm}$ and $\eta_2 = 0.6 \text{ fm}$ are original values and $V_{\text{LS}} \equiv V_{\text{LS1}} = -V_{\text{LS2}}$ is variable parameter in our work. \hat{V}_{Coulomb} is Coulomb potential for the protons.

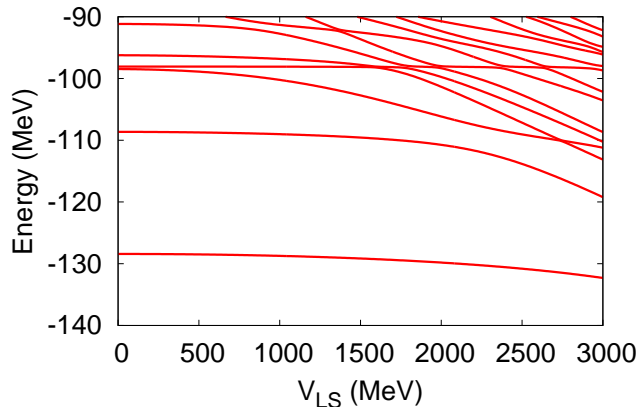


FIG. 3: (Color online) Energy levels of 0^+ states in ^{16}O against the strength of the spin-orbit force, V_{LS} .

III. RESULT AND DISCUSSION

A. Effects of spin-orbit strength

In this section, we discuss the V_{LS} (strength of the spin-orbit force) dependence of the 0^+ energy levels and $E0$ transition matrix elements. The reasonable V_{LS} value of 1600 \sim 2000 MeV has been suggested in the study of scattering phase shift of $\alpha + n$ system [26]. However here we set up two extreme cases of $V_{\text{LS}} = 0$ MeV and 3000 MeV and vary V_{LS} between them to see the tendency of the energy levels and $E0$ transition matrix elements. We discuss the change of the wave functions by calculating squared overlap between the final solution and each basis state.

1. Energy levels

Firstly, we investigate the 0^+ energy levels of ^{16}O . The 0^+ energy levels as a function of the strength of the spin-orbit force, V_{LS} , are shown in Fig. 3. The experimental ground state energy is -127.6 MeV [25]. Here we plot points corresponding to the solution of the Hill-Wheeler equation for each fixed V_{LS} value and connect them with lines in order from bottom. The “ n th state” is defined at each V_{LS} value from the bottom. For $0 \leq V_{\text{LS}} \leq 1500$ MeV, the energies of calculated first and second states are almost independent of V_{LS} . For $V_{\text{LS}} \geq 2000$ MeV, the energy of calculated first state slightly decreases with increasing V_{LS} value; however the second state is much more influenced. This is because the dominant configuration of the ground state is the closed p shell configuration, where the contribution of the spin-orbit force to $p_{3/2}$ and $p_{1/2}$ cancels. On the other hand, in calculated second state, the spin-orbit force acts attractively for the ^{12}C cluster part. In the region slightly above $V_{\text{LS}} = 2000$ MeV, level repulsion of calculated sec-

ond and third states occurs.

Experimentally the 0_2^+ state is observed at $E_x = 6.05$ MeV [12, 13]. However, this excitation energy is calculated to be higher by more than 10 MeV without the spin-orbit force at $V_{\text{LS}} = 0$ MeV. This has been a long standing problem of traditional (microscopic) α cluster models, which cannot take into account the spin-orbit effect. Now this is considerably improved by introducing the dissolution of α clusters.

As discussed later, the main component of the calculated second state at $V_{\text{LS}} = 0$ MeV is four α clusters; even after allowing the dissolution of α clusters, basis states with finite Λ values do not contribute to the calculated second state without spin-orbit force, and ^{12}C cluster part is nothing but three α clusters. It is intriguing to point out that even in the region of $V_{\text{LS}} \geq 2000$ MeV, such four α like state survives and the energy stays almost constant. Finally the four α state becomes calculated fourth state at $V_{\text{LS}} = 3000$ MeV. The result suggests that the four α state is rather decoupled from other states with finite Λ values and survives even after switching on the spin-orbit force.

We also find another example of such decoupling of four α state at -98.1 MeV. At $V_{\text{LS}} = 0$, the calculated state is fourth state. The energy of this state does not change even after increasing V_{LS} . Many level crossings with other states occur; however the character of this state remains at this energy.

2. $E0$ transition matrix element

Next we show the $E0$ transition from the ground state and discuss the effect of α dissolution due to the spin-orbit force. The $E0$ transition matrix element $M(E0, 0_n^+ - 0_1^+)$ from the 0_1^+ to the 0_n^+ state is defined as

$$M(E0, 0_n^+ - 0_1^+) \equiv \left\langle 0_n^+ \left| \sum_{i=1}^{16} e^{\frac{1 + \hat{\tau}_{i3}}{2}} (\hat{\mathbf{r}}_i - \hat{\mathbf{r}}_{\text{c.m.}})^2 \right| 0_1^+ \right\rangle, \quad (7)$$

where $\hat{\mathbf{r}}_{\text{c.m.}} \equiv \frac{1}{16} \sum_{i=1}^{16} \hat{\mathbf{r}}_i$ is the center-of-mass coordinate operator.

The $E0$ transition matrix elements from the first to the second, third and fourth 0^+ states calculated by changing the V_{LS} value, are shown in Fig. 4. Here, n th state is defined from the bottom at each V_{LS} value. For $0 \leq V_{\text{LS}} \leq 1500$ MeV, the $E0$ transition matrix element from the first state to the second state is around $8 e \text{ fm}^2$ almost independent of V_{LS} . This value is much larger than the observed one ($3.55 \pm 0.21 e \text{ fm}^2$). In the region of $V_{\text{LS}} \geq 1500$ MeV, the $E0$ transition matrix element from the first state to the second state decreases. On the other hand, the one from the first 0^+ state to the third 0^+ state increases (the observed value for 0_3^+ is $4.03 \pm 0.09 e \text{ fm}^2$). This is due to the interchanges of the wave functions of the second and third states after their level repulsion.

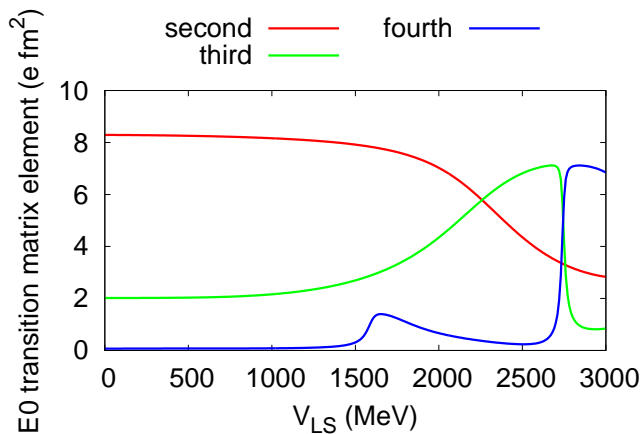


FIG. 4: (Color online) $E0$ transition matrix elements from the first 0^+ state of ^{16}O to the second, third and fourth states calculated in Fig. 3. The horizontal axis is the strength of the spin-orbit force, V_{LS} .

Why these changes influence the $E0$ transition probability will be discussed later in detail. Experimentally the transition matrix element to the third 0^+ state is slightly larger than one for the second 0^+ state, and this is realized in our model with the V_{LS} value slightly above 2000 MeV.

3. Squared overlap

In this subsection, the wave function of each state is analyzed in more detail. The squared overlap between the final solution, $|\Phi\rangle$ in Fig. 3, and each basis state, $|\Psi_{ijk}\rangle$ in Eqs. (2) and (3), at fixed V_{LS} value is defined as

$$\left| \frac{\langle \Psi_{ijk} | \Phi \rangle}{\sqrt{\langle \Psi_{ijk} | \Psi_{ijk} \rangle} \sqrt{\langle \Phi | \Phi \rangle}} \right|^2, \quad (8)$$

and we compare the squared overlaps for the cases of $V_{\text{LS}} = 0$ MeV and $V_{\text{LS}} = 3000$ MeV.

We start with the case without the spin-orbit force ($V_{\text{LS}} = 0$ MeV). The squared overlap between the first state calculated at $V_{\text{LS}} = 0$ MeV in Fig. 3 and $|\Psi_{ijk}\rangle$ is shown in Fig. 5. Figures 5 (a), (b), (c) and (d) are the squared overlaps with $\Lambda = 0, 1/3, 2/3$ and 1 basis states, respectively. The first state is obtained to be a compact tetrahedral structure (small h and R), and $\Lambda = 0$ gives the largest squared overlap.

The squared overlap between the second state calculated at $V_{\text{LS}} = 0$ MeV in Fig. 3 and $|\Psi_{ijk}\rangle$ is shown in Fig. 6. Figures 6 (a), (b), (c) and (d) are the squared overlaps with $\Lambda = 0, 1/3, 2/3$ and 1 basis states, respectively. In this case, spatially expanded triangular pyramid structures (large R and h) with $\Lambda = 0$ are the dominant configurations. Without the spin-orbit force at $V_{\text{LS}} = 0$ MeV, both the first and second states are

obtained to have four α configurations, although their spatial extensions are quite different.

Next we discuss the cases calculated with extreme spin-orbit strength ($V_{\text{LS}} = 3000$ MeV). The squared overlap between the first state calculated at $V_{\text{LS}} = 3000$ MeV in Fig. 3 and $|\Psi_{ijk}\rangle$ is shown in Fig. 7. Figures 7 (a), (b), (c) and (d) are the squared overlaps with $\Lambda = 0, 1/3, 2/3$ and 1 basis states, respectively. Comparing with the case of $V_{\text{LS}} = 0$ MeV, still compact tetrahedral structures (small R and h) are important, but the squared overlap with $\Lambda > 0$ basis states are much increased as seen in Figs. 7 (b), (c), and (d).

Finally, the squared overlap between the second state calculated at $V_{\text{LS}} = 3000$ MeV in Fig. 3 and $|\Psi_{ijk}\rangle$ is shown in Fig. 8. Figures 8 (a), (b), (c) and (d) are the squared overlaps with $\Lambda = 0, 1/3, 2/3$ and 1 basis states, respectively. In this case, the optimal h value is rather large, but R is small and basis states with $\Lambda=1$ play a dominant role. Thus the subclosure configuration of $p_{3/2}$ is realized in ^{12}C . The second state calculated at $V_{\text{LS}} = 0$ MeV and that at $V_{\text{LS}} = 3000$ MeV are significantly different, and this difference affects the $E0$ transition as discussed in detail from now.

B. Mechanism for the $E0$ transition suppression

In this subsection, we discuss how the level repulsion and interchange of the wave functions between the second and third states calculated in Fig. 3 affect the $E0$ transition probability from the first state. We focus on the change of the wave function of the second state, especially for the change of ^{12}C cluster part from three α clusters to the $p_{3/2}$ subclosure of the jj -coupling shell model.

1. $E0$ transition between two typical basis states

To discuss the change of the $E0$ transition probability, firstly we prepare typical basis states representing the characters of the first and second states obtained in Fig. 3 and investigate the change of $E0$ transition matrix element. We introduce initial and final states. The initial state, Ψ_i , represents the first state of Fig. 3 and has compact tetrahedral structure. The final state, Ψ_f , represents the second state of Fig. 3 and has $^{12}\text{C} + \alpha$ structure. We define the initial state as $\Psi_i \equiv \Psi(R = 0.1 \text{ fm}, h = \sqrt{2/3} \times 0.1 \text{ fm}, \Lambda = 0)$ and the final state as $\Psi_f \equiv \Psi(R = 0.1 \text{ fm}, h = \sqrt{2/3} \times 5.0 \text{ fm}, \Lambda = \Lambda_f)$. Here Λ_f is a control parameter, which changes the ^{12}C cluster part from three α to the subclosure of $p_{3/2}$ orbits. Indeed, Ψ_f with $\Lambda_f = 1$ is the dominant basis state for the second state of Fig. 3, when the strength of the spin-orbit force is $V_{\text{LS}} = 3000$ MeV.

The $E0$ transition matrix element between the initial state Ψ_i and the final state Ψ_f is shown in Fig. 9 as a function of Λ_f . At $\Lambda_f = 0$, the calculated $E0$ transition

matrix element is $20.1 e \text{ fm}^2$. The value is about six times compared with the experimental one [12, 13]. However, this $E0$ transition matrix element drastically decreases with increasing Λ_f , and the value becomes comparable to the experiments around $\Lambda_f = 1$.

As a mechanism to explain this drastic decrease of the $E0$ transition matrix element to the second 0^+ state, we take notice on the change of the intrinsic spin structure in the final state. The initial state is compact four α state, which agrees with the closed p shell configuration, and the state has intrinsic spin equal to zero independent of the Λ value. However the final state is $^{12}\text{C} + \alpha$ cluster state, and when $\Lambda_f > 0$, quasi α clusters can have finite expectation values of the intrinsic spin unlike α clusters. Since the $E0$ transition operator does not contain the spin part, it cannot connect two states with different intrinsic spin structures.

The intrinsic spin operator \hat{S} is defined as

$$\hat{S} = \sum_{i=1}^{16} \hat{s}_i, \quad (9)$$

where \hat{s}_i is the spin operator for the i th nucleon. Figure 10 shows the expectation value of the square of this operator as functions of R and h . Figure 10 (a) is the case of $\Lambda = 0$, and the values are exactly zero independent on R and h values, because each α cluster has spin zero [27]. On the contrary, Fig. 10 (b) shows the case of $\Lambda = 1$, and the values become finite except for the region of very small R and h values. Although we do not change the spin part of the wave function, the total system has finite intrinsic spin owing to the parameter Λ given to the spatial part. The expectation value of squared intrinsic spin for the final state with $\Lambda_f = 1$, which is the dominant basis state for the second state calculated with $V_{\text{LS}} = 3000 \text{ MeV}$, is 2.6. Since the value for the ground state is almost zero, the two states have quite different spin structures. The $E0$ transition operator does not act on the spin part, thus the $E0$ transition between two states which have different spin values is suppressed. In Fig. 10 (b), the expectation value of squared spin numerically converge to $2.66\dots \approx 8/3$ at the limit of $R \rightarrow 0$ when h value is large enough.

2. Intrinsic spin of the full solutions

Next, we discuss the intrinsic spin of the full solution. The expectation value of the square of the intrinsic spin operator for the full solutions obtained in Fig. 3, are shown in Table I. At $V_{\text{LS}} = 0 \text{ MeV}$, all the 0^+ states listed here have the value close to zero. With increasing V_{LS} , the basis states with finite Λ start contributing to each state, and the intrinsic spin increases in all the states listed here. However the increase is much smaller in the ground state due to the closed shell structure of the p shell; the state has the value of 0.3 at $V_{\text{LS}} = 3000 \text{ MeV}$. On the other hand, the value for the second 0^+

TABLE I: The expectation value of the square of the intrinsic spin operator for the 0^+ states of ^{16}O obtained in Fig. 3. Here V_{LS} stands for the strength of the spin-orbit force in the Hamiltonian.

$V_{\text{LS}} \text{ (MeV)}$	0	500	1000	1500	2000	2500	3000
0_1^+	0.0	0.0	0.0	0.1	0.1	0.2	0.3
0_2^+	0.0	0.0	0.1	0.1	0.4	1.2	1.8
0_3^+	0.0	0.1	0.3	0.7	0.9	0.6	1.9
0_4^+	0.0	0.0	0.0	0.0	1.8	1.9	0.7

state is 1.8, where the subclosure configuration of the $p_{3/2}$ shell for the ^{12}C cluster part is important. The intrinsic spin structure of these two states are completely different. This is the reason for the suppression of the $E0$ transition probability between these states. Although the $E0$ operator itself does not have the spin dependence, the matrix element is sensitive to the difference of intrinsic spin structures of the two states.

C. Orientation of ^{12}C

In our model, we considered only triangular pyramid structures, *i.e.* we did not consider the effect of rotation of three α clusters forming ^{12}C with respect to the last α cluster. The definition of the coordinate system in this work may lead to the overestimation of the $E0$ transition strength. Taking into account other orientations of ^{12}C as in the previous study [17] is expected to help in better reproduction of the experimental value.

For instance, in Fig. 4, the $E0$ transition matrix elements from the first to the second 0^+ states is around $8.3 e \text{ fm}^2$ at $V_{\text{LS}} = 0 \text{ MeV}$. This value is reduced when other orientations of ^{12}C are introduced. If we prepare $\Lambda = 0$ (four α) wave functions with other orientations of ^{12}C with respect to the fourth α and diagonalize the Hamiltonian, the value decreases to $6.9 e \text{ fm}^2$. In our analyses we needed rather large value of $V_{\text{LS}} \sim 2500 \text{ MeV}$ to reproduce the experimental $E0$ value from the ground to the second 0^+ state; however this result indicates that we could reproduce it with a bit smaller V_{LS} value when this orientation effect is taken into account.

IV. CONCLUSION

In this study, for ^{16}O , the 0^+ energy levels and the $E0$ transition matrix elements from the ground state have been investigated in the framework of AQCM. The $E0$ transition strength has been known as a quantity which characterizes the cluster structure of low-lying excited states, and here we focused on the dependence on the strength of the spin-orbit force, V_{LS} .

The ground state is compact four α state and almost independent of V_{LS} . On the contrary, as pointed out by many previous works, cluster structure is important in

the 0_2^+ state, and this is obtained also in our model. In addition, in the present study we discussed the change of the wave function of the ^{12}C cluster part. With increasing V_{LS} , the level repulsion occurs and the ^{12}C cluster part change from three α 's, which are not affected by the spin-orbit force, to the $p_{3/2}$ subclosure of the jj -coupling shell model, and the excitation energy of the 0_2^+ state drastically decreases.

The $E0$ transition matrix elements from the ground state to the excited states are strongly dependent on the level repulsions. For $0 \leq V_{\text{LS}} \leq 1500$ MeV, the $E0$ transition matrix element from the ground state to the second 0^+ state is around $8 e \text{ fm}^2$, which is much larger than the observed one ($3.55 \pm 0.21 e \text{ fm}^2$). In the region of $V_{\text{LS}} \geq 1500$ MeV, it starts decreasing and becomes comparable to the experimental one slightly above $V_{\text{LS}} = 2000$ MeV. On the other hand, the value from the ground state to the third 0^+ state is around $2 e \text{ fm}^2$ at $V_{\text{LS}} = 0$ MeV and this is too small compared with the experimental value of $4.03 \pm 0.09 e \text{ fm}^2$. The value increases and becomes comparable to the experimental one around $V_{\text{LS}} = 2000$ MeV. The decrease of the transition matrix element to the second 0^+ and the increase to the third 0^+ state is due to the level repulsion between the second and third states. The wave functions of these states are interchanged. Experimentally the transition matrix element to the third 0^+ state is slightly larger than one for the second 0^+ state, and this is realized with the V_{LS} value slightly above 2000 MeV. In this model, only triangular pyramid structure of ^{16}O has been considered; however taking into account other orientations of ^{12}C part with respect to α is expected to help in further reproduction of the experimental transition matrix elements.

The expectation value of the square of the intrinsic spin was also analyzed. At $V_{\text{LS}} = 0$ MeV, the ground and sec-

ond 0^+ states have the value close to zero. With increasing V_{LS} , the basis states with finite A start contributing to each state, and the intrinsic spin increases; however the increase is much smaller in the ground state due to the closed shell structure of the p shell (the value is 0.3 at $V_{\text{LS}} = 3000$ MeV). On the other hand, at $V_{\text{LS}} = 3000$ MeV, the value for the second 0^+ state is 1.8, where the subclosure configuration of the $p_{3/2}$ shell for the ^{12}C cluster part is important. The intrinsic spin structure of these two states are completely different. This is the reason for the suppression of the $E0$ transition probability between these states. Although the $E0$ operator itself does not have the spin dependence, the matrix element is sensitive to the difference of intrinsic spin structures of the two states.

In the traditional microscopic α cluster models, there has been a long standing problem that the calculated excitation energy of 0_2^+ is higher than the experiments by more than 10 MeV, since the spin-orbit force is missing. Now this is considerably improved by introducing the dissolution of α clusters. However, taking into account other effect, such as three-body force effect [28], would be promising in order to fully solve the problem.

In this study we found an important correlation between the strength of the spin-orbit force and $E0$ transition to low-lying excited states. The $E0$ transition is sensitive to the persistence of $N\alpha$ correlation in the excited states and can be its measure. Similar investigations for other light nuclei are on going.

Acknowledgments

The authors would like to thank T. Ichikawa for the discussions.

-
- [1] T. Kawabata *et al.*, Phys. Lett. B **646**, 6 (2007).
 - [2] Y. Sasamoto *et al.*, Mod. Phys. Lett. A **21**, 2393 (2006).
 - [3] T. Yoshida, N. Itagaki, and T. Otsuka, Phys. Rev. C **79**, 034308 (2009).
 - [4] Taiichi Yamada and Yasuro Funaki, Phys. Rev. C **92**, 034326 (2015).
 - [5] T. Ichikawa, N. Itagaki, T. Kawabata, Tz. Kokalova and W. von Oertzen, Phys. Rev. C **83**, 061301(R) (2011).
 - [6] T. Ichikawa, N. Itagaki, Y. Kanada-En'yo, Tz. Kokalova, and W. von Oertzen, Phys. Rev. C **86**, 031303(R) (2012).
 - [7] H. Horiuchi and K. Ikeda, Prog. Theor. Phys. **40**, 277 (1968).
 - [8] A. Arima, H. Horiuchi, and T. Sebe, Phys. Lett. B **24**, 129 (1967).
 - [9] W. C. Haxton and Calvin Johnson, Phys. Rev. Lett. **65** 1325 (1990).
 - [10] Y.-W. Lui, H. L. Clark, and D. H. Youngblood, Phys. Rev. C **64**, 064308 (2001).
 - [11] Z. Ma, N. Van Giai, H. Toki, and M. L'Huillier, Phys. Rev. C **55**, 2385 (1997).
 - [12] F. Ajzenberg-Selove, Nucl. Phys. A **460**, 1 (1986).
 - [13] D. R. Tilley, H. R. Weller, and C. M. Cheves, Nucl. Phys. A **564**, 1 (1993).
 - [14] T. Yamada, Y. Funaki, H. Horiuchi, K. Ikeda, and A. Tohsaki, Prog. Theor. Phys. **120**, 1139 (2008).
 - [15] Y. Suzuki, Prog. Theor. Phys. **55**, 1751 (1976); **56**, 111 (1976).
 - [16] T. Yamada, Y. Funaki, T. Myo, H. Horiuchi, K. Ikeda, G. Röpke, P. Schuck, and A. Tohsaki, Phys. Rev. C **85**, 034315 (2012).
 - [17] Y. Kanada-En'yo, Phys. Rev. C **89**, 024302 (2014).
 - [18] B. F. Bayman and A. Bohr, Nucl. Phys. **9**, 596 (1958/59).
 - [19] T. Suhara, N. Itagaki, J. Cseh, and M. Płoszajczak, Phys. Rev. C **87**, 054334 (2013).
 - [20] N. Itagaki, H. Masui, M. Ito, and S. Aoyama, Phys. Rev. C **71**, 064307 (2005).
 - [21] H. Masui and N. Itagaki, Phys. Rev. C **75** 054309 (2007).
 - [22] N. Itagaki, J. Cseh, and M. Płoszajczak, Phys. Rev. C **83**, 014302 (2011).
 - [23] A. B. Volkov, Nucl. Phys. **74**, 33 (1965).
 - [24] R. Tamagaki, Prog. Theor. Phys. **39**, 91 (1968).
 - [25] National Nuclear Data Center <http://www.nndc.bnl.gov>

- [26] S. Okabe and Y. Abe, *Prog. Theor. Phys.* **61**, 1049 (1979).
- [27] D. M. Brink, in *Proceedings of the International School of Physics "Enrico Fermi,"* Course XXXVI, edited by C. Bloch (Academic, New York, 1966), p. 247.
- [28] Naoyuki Itagaki, Akira Ohnishi, and Kiyoshi Kato, *Prog. Theor. Phys.* **94**, 1019 (1995).

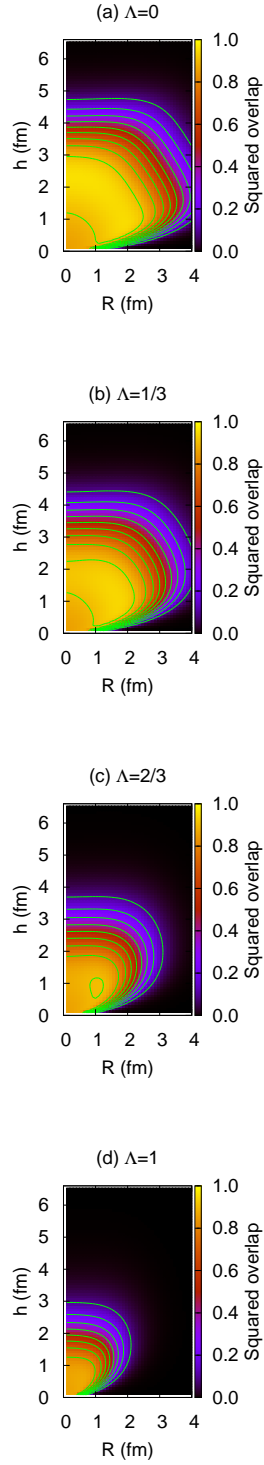


FIG. 5: (Color online) Squared overlap between the first state calculated at $V_{LS} = 0$ MeV in Fig. 3 and the basis state $|\psi(R, h, \Lambda)\rangle$.

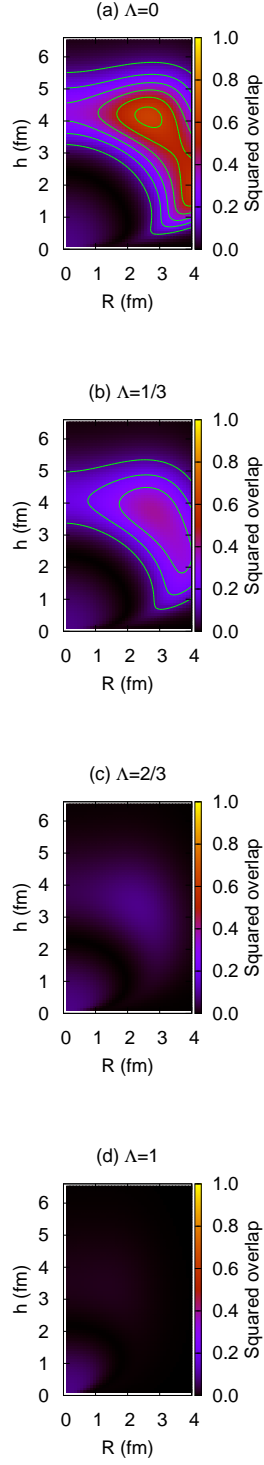


FIG. 6: (Color online) Squared overlap between the second state calculated at $V_{LS} = 0$ MeV in Fig. 3 and the basis state $|\Psi(R, h, \Lambda)\rangle$.

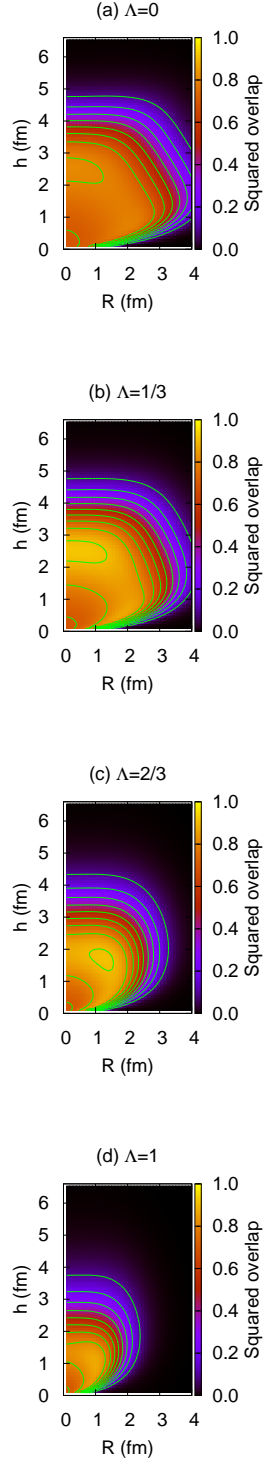


FIG. 7: (Color online) Squared overlap between the first state calculated at $V_{LS} = 3000$ MeV in Fig. 3 and the basis state $|\psi(R, h, \Lambda)\rangle$.

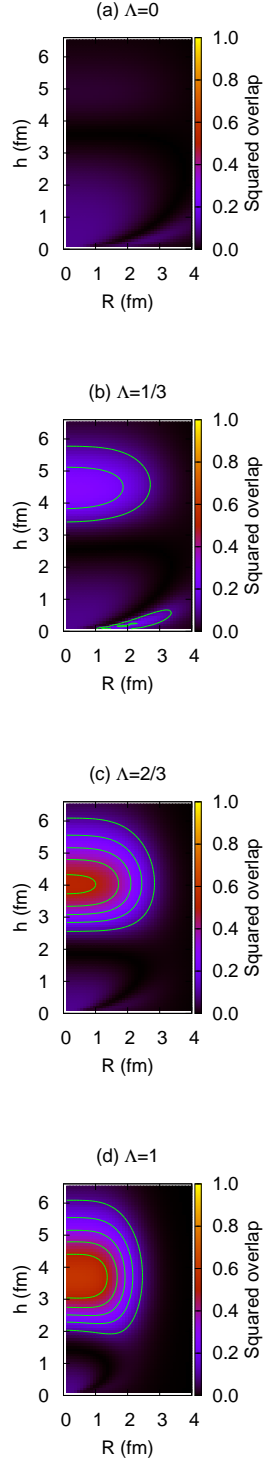


FIG. 8: (Color online) Squared overlap between the second state calculated at $V_{LS} = 3000$ MeV in Fig. 3 and the basis state $|\Psi(R, h, \Lambda)\rangle$.

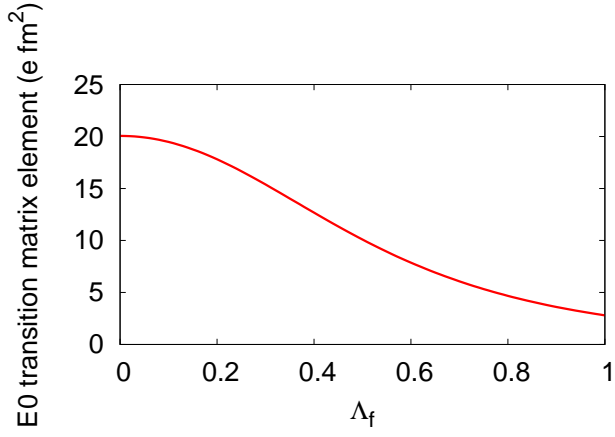


FIG. 9: (Color online) $E0$ transition matrix element between the compact four α state with $\Psi(R = 0.1 \text{ fm}, h = \sqrt{2/3} \times 0.1 \text{ fm}, \Lambda = 0)$ and typical $^{12}\text{C} + \alpha$ cluster state $\Psi(R = 0.1 \text{ fm}, h = \sqrt{2/3} \times 5.0 \text{ fm}, \Lambda = \Lambda_f)$ as a function of Λ_f .

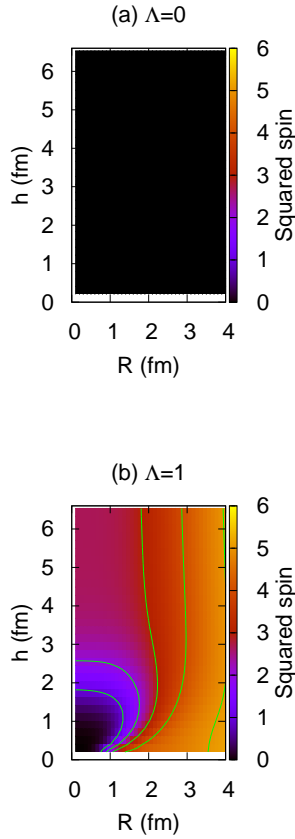


FIG. 10: (Color online) The expectation value of squared spin at (a) $\Lambda = 0$ and (b) $\Lambda = 1$ for the basis state $|\Psi(R, h, \Lambda)\rangle$.